The structure and molecular properties of the acetylene–HCN complex as determined from the rotational spectra

P. D. Aldrich, S. G. Kukolich, and E. J. Campbell

Citation: The Journal of Chemical Physics **78**, 3521 (1983); doi: 10.1063/1.445175
View online: http://dx.doi.org/10.1063/1.445175
View Table of Contents: http://scitation.aip.org/content/aip/journal/jcp/78/6?ver=pdfcov
Published by the AIP Publishing

The structure and molecular properties of the acetylene–HCN complex as determined from the rotational spectra

P. D. Aldrich, S. G. Kukolich, and E. J. Campbell

Noyes Chemical Laboratory, University of Illinois, Urbana, Illinois 61801
(Received 2 August 1982; accepted 10 September 1982)

The microwave spectra for four isotopic species of a complex formed between acetylene and HCN have been obtained using the pulsed, Fourier-transform method with gas pulsed into an evacuated Fabry–Perot cavity. The spectra indicate the complex to be a T-shaped near-prolate asymmetric rotor ($\kappa = -0.993$) in its ground vibrational state in which HCN lies on the C_2 symmetry axis with the hydrogen atom of HCN pointing to the middle of the triple bond of acetylene. The carbon atom of HCN is situated 3.656 Å from the acetylene center of mass. Nuclear quadrupole coupling constants for N are obtained for all four isotopes and deuterium quadrupole coupling constants are obtained for two isotopes. Various contributions to the electric field gradients at quadrupolar nuclei are discussed.

I. INTRODUCTION

Recently, we have measured the high resolution, ground vibrational state microwave spectra of many hydrogen-bound complexes formed between simple unsaturated hydrocarbons and hydrogen halides.[1–9] In all molecules examined they are near prolate asymmetric rotors with the hydrogen bond formed between the π electron system of the hydrocarbon and the electrophilic hydrogen atom of the hydrogen halide. These complexes are of great chemical interest as their structures are often suggestive of intermediates whereby addition of hydrogen halides to unsaturated hydrocarbon systems proceeds. In the case of the ethylene dimers, the complex may be a precursor to carbonium ion formation. Furthermore, the properties of these complexes help to elucidate the nature of the hydrogen bond especially in the expanded sense of any low energy, electrostatic bond formed between an electropositive hydrogen atom and an electron-rich, nucleophilic region. Hydrogen cyanide is a weak acid and is quite capable of hydrogen bond formation as both a proton donor and proton acceptor.[10–12] It is thus interesting to see if HCN will readily form a complex analagous to the acetylene–HF, acetylene–HCl complexes, with acetylene as a proton acceptor, and have similar properties. In acetylene–HCl, the Cl nuclear quadrupole coupling constant gave evidence for the hydrogen atom of HCl experiencing an anisotropic potential.[2] The nitrogen quadrupole coupling constant can also help establish this in the acetylene–HCN dimer as well as whether or not the electronic environment at the nitrogen atom is perturbed by complex formation. Two sites for deuterium isotopic substitution exist to also measure these effects elsewhere in the dimer.

II. EXPERIMENTAL

The details of the spectrometer employed for this work have been given in great detail previously.[13,14] The acetylene–HCN dimers were generated by expanding a gas mixture of ~2% of both acetylene and HCN in argon at room temperature and 0.5–2.5 atm through a solenoid valve with a 0.5 mm diameter nozzle opening into a Fabry–Perot cavity which is at $\sim 10^{-5}$ Torr. All rotational transitions within the cavity bandwidth (~1 MHz) were then polarized by a suitably delayed 3.0 μs microwave power pulse. The resulting coherent molecular emission time domain signal is subsequently digitized at a rate of 0.5 μs per point for 256 points. Approximately 20 signals are then taken at a rate of ~1 Hz with every alternate signal, which is taken with no gas in the cavity, subtracted from the average to eliminate any coherent noise. The averaged signal is then Fourier transformed to give the power spectrum which consists of 256 points at 3.9 kHz per point resolution. A characteristic Doppler doubling is present in the frequency spectrum varying from 5–30 kHz with the actual molecular resonance located at the midpoint of the two Doppler components. This phenomenon is well understood and has been described in detail elsewhere.[15] The half-widths at half-height are typically ~6 kHz. The HCN used was supplied by Fumico and the acetylene was supplied by Matheson. DCN was prepared by dripping concentrated deuterated orthophosphoric acid on KCN and condensing the gas evolved *in vacuo*. Acetylene-d_2 was prepared by dripping D_2O on calcium carbide and condensing the gas *in vacuo*.

Four a-dipole, R branches between 3 and 17 GHz were obtained for the $H\,^{12}C\,^{12}CH–H\,^{12}C\,^{14}N$ and $H\,^{12}C\,^{12}CH–D\,^{12}C\,^{14}N$ isotopic species in their ground vibrational states. The $1_{01} \leftarrow 2_{02}$ and $2_{02} \leftarrow 3_{03}$ transitions were obtained for $H\,^{12}C\,^{13}CH–H\,^{12}C\,^{14}N$ in natural abundance. The $0_{00} \leftarrow 1_{01}$, $1_{01} \leftarrow 2_{02}$, and $1_{10} \leftarrow 2_{11}$ transitions were observed for $D\,^{12}C\,^{12}CD–H\,^{12}C\,^{14}N$.

III. RESULTS

A. Determination of molecular constants

The hyperfine components for the $J = 0 \leftarrow 1$, $J = 1 \leftarrow 2$, $J = 2 \leftarrow 3$, and $J = 3 \leftarrow 4$ rotational transitions are listed in Table I for the $H\,^{12}C\,^{12}CH–H\,^{12}C\,^{14}N$ isotopic species. These data were reduced in a two-step procedure in which the hyperfine structure is first fit to give the nitrogen nuclear quadrupole constants χ^N_{aa} and χ^N_{bb} and the unperturbed rotational transitions. This fit ignores

 0021-9606/83/063521-10$2.10

TABLE I. Observed and calculated transition frequencies for $H^{12}C^{12}CH-H^{12}C^{14}N$.

$J_{K_{-1}K_{+1}} \rightarrow J'_{K'_{-1}K'_{+1}}$	$F \rightarrow F'$	Observed (MHz)	Calculated (MHz)	Difference (kHz)
$0_{00} \rightarrow 1_{01}$	1 → 1	3984.230	3984.229	+1
	1 → 2	3985.544	3985.544	0
	1 → 0	3987.515	3987.516	−1
$1_{11} \rightarrow 2_{12}$	1 → 2	7846.684	7846.684	0
	2 → 2	7847.341	7847.342	−1
	1 → 1	7847.778	7847.778	0
	2 → 3	7848.047	7848.046	+1
	0 → 1	7849.424	7849.424	0
$1_{01} \rightarrow 2_{02}$	2 → 2	7968.892	7968.893	−1
	0 → 1	7969.116	7969.112	+4
	1 → 2	7970.208	7970.208	0
	2 → 3	7970.302	7970.302	0
	1 → 1	7972.397	7972.399	−2
$2_{12} \rightarrow 3_{13}$	2 → 3	11770.914	11770.914	0
	3 → 4	11771.305	11771.306	−1
	2 → 2	11772.393	11772.392	+1
$2_{02} \rightarrow 3_{03}$	1 → 2	11953.990	11953.988	+2
	2 → 3	11954.209	11954.207	+2
	3 → 4	11954.258	11954.259	−1
	2 → 2	11956.179	11956.179	0
	3 → 3	11952.795	11952.798	−3
$2_{11} \rightarrow 3_{12}$	2 → 3	12132.851	12132.848	−3
	3 → 4	12133.244	12133.239	+5
	3 → 3	12132.138	12132.143	−5
	2 → 2	12134.326	12134.328	−2
$3_{13} \rightarrow 4_{14}$	3 → 4	15693.919	15693.918	+1
	2 → 3	15694.037	15694.036	+1
	4 → 5	15694.090	15694.092	−2
$3_{03} \rightarrow 4_{04}$	2 → 3	15936.789	15936.789	0
	3 → 4	15936.881	15936.883	−2
	4 → 5	15936.918	15936.915	+3
$3_{12} \rightarrow 4_{13}$	3 → 4	16176.408	16176.408	0
	2 → 3	16176.526	16176.525	+1
	4 → 5	16176.582	16176.582	0

the small 2nd and higher order effects of the nitrogen quadrupole interaction which are small and utilizes the equation

$$\nu_{ob} = C_a \chi^N_{aa} + C_b \chi^N_{bb} + \nu_0 \,, \tag{1}$$

where ν_0 is the unperturbed rotational frequency and C_a and C_b are given by

$$C_g = \frac{1}{h}\left[f' \frac{2J'+3}{J'}(\alpha'^2_{gz} - \alpha'^2_{cz}) - f \frac{2J+3}{J}(\alpha^2_{gz} - \alpha^2_{cz})\right] \,, \quad g = a, b \,. \tag{2}$$

Here, f' and f are Casmir's function for the upper and lower state and α'^2_{gz} and α^2_{gz} are the squares of the direction cosines between the z axis and the g principal axis averaged over the upper and lower asymmetric rotor wave functions. Because of the limited number of rotational transitions observed, the unperturbed rotational line centers were then fit to a rotational Hamiltonian that included a symmetric top centrifugal distortion analysis. This two-step procedure prevents the errors resulting from the limited centrifugal distortion treatment, which amount to as much as 27 kHz for a given rotational transition, from entering into the determination of χ^N_{aa} and χ^N_{bb}. The differences given in Table I reflect the accuracy of the first step of this procedure and average about 2 kHz. A similar procedure was used for the $J = 2 \rightarrow 3$ and $J = 3 \rightarrow 4$ hyperfine transitions of $H^{12}C^{12}CH-D^{12}C^{14}N$ given in Table II. For these transitions, the effects of a deuterium quadrupole could be ignored with only a small loss of accuracy and thus $I = 1$ for all of these transitions in Table II. The $H^{13}C^{12}CH-H^{12}C^{14}N$ hyperfine components in Table III were also reduced using Eq. (1) and Eq. (2).

For the $0_{00} \rightarrow 1_{01}$, $1_{11} \rightarrow 2_{12}$, $1_{01} \rightarrow 2_{02}$, and $1_{10} \rightarrow 2_{11}$ rotational transitions in $H^{12}C^{12}CH-D^{12}C^{14}N$ the deuterium quadrupole effects were clearly resolved. The Hamiltonian

$$\mathcal{H} = \mathcal{H}_{\rm rot} + \mathbf{Q}(\mathrm{N}) : \mathbf{V}(\mathrm{N}) + \mathbf{Q}(\mathrm{D}) : \mathbf{V}(\mathrm{D}) \tag{3}$$

was used where $\mathbf{Q}$ and $\mathbf{V}$ are the nuclear quadrupole and electric field gradient tensors for either nitrogen or deuterium. Matrix elements are computed in the basis

$$\mathbf{I}_N + \mathbf{I}_D = \mathbf{I} \,, \quad \mathbf{I} + \mathbf{J} = \mathbf{F} \,. \tag{4}$$

TABLE II. Observed and calculated transition frequencies for $H\,^{12}C\,^{12}CH-D\,^{12}C\,^{14}N$.

$J_{K_{-1}K_{+1}} \rightarrow J'_{K'_{-1}K'_{+1}}$	$I, F \rightarrow I', F'$	Observed (MHz)	Calculated (MHz)	Difference (kHz)
$0_{00} \rightarrow 1_{01}$	2,2 → 0,1	3 981.846(4)	3 981.850	−4
	2,2 → 2,2	3 981.881(2)	3 981.879	+2
	1,1 → 1,0	3 981.914(3)	3 981.920	−6
	0,0 → 1,1	3 983.162(3)	3 983.168	−6
	2,2 → 2,3	3 983.197(2)	3 983.190	+7
	1,1 → 1,2	3 983.228(2)	3 983.231	−3
	2,2 → 2,1	3 985.186(1)	3 985.185	+1
$1_{11} \rightarrow 2_{12}$	0,1 → 2,2	7 842.452(2)	7 842.450	+2
	2,3 → 2,3	7 843.107(2)	7 843.107	0
	1,2 → 2,2	7 843.140(4)	7 843.142	−2
	2,2 → 0,2	7 843.556(2)	7 843.556	0
	1,1 → 1,2	7 843.792(3)	7 843.793	−1
	2,3 → 2,4	7 843.815(2)	7 843.813	+2
	1,2 → 1,3	7 843.858(3)	7 843.859	−1
$1_{01} \rightarrow 2_{02}$	1,2 → 2,2	7 964.186(4)	7 964.187	−1
	2,3 → 2,3	7 964.200(3)	7 964.199	+1
	2,1 → 0,2	7 964.411(3)	7 964.413	−2
	2,1 → 2,1	7 964.444(3)	7 964.440	+4
	2,2 → 2,3	7 965.511(3)	7 965.510	+1
	2,3 → 2,4	7 965.611(3)	7 965.612	−1
	1,2 → 1,3	7 965.619(4)	7 965.622	−3
	1,0 → 2,1	7 967.703(5)	7 967.705	−2
	2,2 → 0,2	7 967.719(3)	7 967.719	0
	0,1 → 0,2	7 967.752(9)	7 967.748	+4
$1_{10} \rightarrow 2_{11}$	2,2 → 2,2	8 083.049(2)	8 083.049	0
	0,1 → 2,2	8 083.064(2)	8 083.063	+1
	1,1 → 1,2	8 084.387(2)	8 084.390	−3
	2,3 → 2,4	8 084.411(3)	8 084.410	+1
	1,2 → 1,3	8 084.460(3)	8 084.457	+3
	2,1 → 0,2	8 085.805(2)	8 085.806	−1
	2,1 → 2,1	8 085.822(3)	8 085.820	+2
$2_{12} \rightarrow 3_{13}$ [a]	1,2 → 1,3	11 764.578	11 764.578	0
	1,3 → 1,4	11 764.978	11 764.978	0
$2_{02} \rightarrow 3_{03}$ [a]	1,1 → 1,2	11 946.960	11 946.962	−2
	1,3 → 1,4	11 947.241	11 947.239	+2
$2_{11} \rightarrow 3_{12}$ [a]	1,2 → 1,3	12 125.426	12 125.425	+1
	1,3 → 1,4	12 125.823	12 125.824	−1
$3_{13} \rightarrow 4_{14}$ [a]	1,3 → 1,4	15 685.482	15 685.483	−1
	1,2 → 1,3	15 685.608	15 685.603	+5
	1,4 → 1,5	15 685.657	15 685.660	−3

[a]Deuterium nuclear quadrupole interaction not considered.

A value for A was assumed from a fit of the $J=2\rightarrow 3$ and $J=3\rightarrow 4$ unperturbed line centers and B, C, D_J, and D_{JK} were fit along with χ^N_{aa}, χ^N_{bb}, χ^D_{aa}, and χ^D_{bb}. A weighted nonlinear least squares program was used in which a weight of $1/\sigma_i^2$ was assigned to each transition where σ_i is the standard deviation of the measurement given in parentheses after each measurement in Table II. Because four rotational parameters are fit to four rotational transitions, the values obtained for B, C, D_J, and D_{JK} are useful only for calculating line centers from the analytical expressions for the $0_{00}\rightarrow 1_{01}$, $1_{11}\rightarrow 2_{12}$, $1_{01}\rightarrow 2_{02}$, and $1_{10}\rightarrow 2_{11}$ transitions given elsewhere.[4]

The $1_{01}\rightarrow 2_{02}$ and $1_{10}\rightarrow 2_{11}$ transitions of $D\,^{12}C\,^{12}CD-H\,^{12}C\,^{14}N$ were fit according to Eqs. (1) and (2) ignoring the deuterium hyperfine components. The $0_{00}\rightarrow 1_{01}$ transition of $D\,^{12}C\,^{12}CD-H\,^{12}C\,^{14}N$ was resolved into its deuterium quadrupole hyperfine components which are listed in Table IV along with the standard deviation σ_i of the measurements. These components were fit using Eq. (3) where a third term is added for the second deuterium nuclear quadrupole interaction in the basis

$$\mathbf{J}+\mathbf{I}_{D_1}=\mathbf{F}_1\ ,$$
$$\mathbf{F}_1+\mathbf{I}_{D_2}=\mathbf{F}_2\ , \tag{5}$$
$$\mathbf{F}_2+\mathbf{I}_N=\mathbf{F}\ .$$

A weight of $1/\sigma_i^2$ was assigned to each transition and matrix elements off-diagonal in J were ignored. The advantage to this coupling scheme lies in the fact that for $J=0$, the F_2 quantum number is actually the I_D quantum number where

$$\mathbf{I}_{D_1}+\mathbf{I}_{D_2}=\mathbf{I}_D\ , \tag{6}$$

thus identifying the symmetry of the spin states. The

TABLE III. Observed and calculated transition frequencies for $H^{12}C^{13}CH-H^{12}C^{14}N$.

$J_{K_{-1}K_{+1}} \rightarrow J'_{K'_{-1}K'_{+1}}$	$F \rightarrow F'$	Observed (MHz)	Calculated (MHz)	Difference (kHz)
$1_{01} \rightarrow 2_{02}$	2 → 2	7 824.990	7 824.993	−3
	0 → 1	7 825.211	7 825.208	+3
	1 → 2	7 826.314	7 826.309	+5
	2 → 3	7 826.395	7 826.400	−5
$2_{02} \rightarrow 3_{03}$	1 → 2	11 738.146	11 738.144	+2
	2 → 3	11 738.368	11 738.368	0
	3 → 4	11 738.415	11 738.416	−1

TABLE IV. Observed and calculated transition frequencies for $D^{12}C^{12}CD-H^{12}C^{14}N$.

$J_{K_{-1}K_{+1}} \rightarrow J'_{K'_{-1}K'_{+1}}$	$F_1, F_2, F \rightarrow F'_1, F'_2, F'$	Observed (MHz)	Calculated (MHz)	Difference (kHz)
$0_{00} \rightarrow 1_{01}$ [a]	1, 2, 2 → 2, 1, 1	3813.2006(52)	3813.2074	−6.8
	1, 2, 3 → 2, 3, 3	3813.2330(17)	3813.2360	−3.0
	1, 2, 3 → 1, 2, 2	3813.2634(20)	3813.2589	4.5
	1, 0, 1 → 1, 1, 2	3814.5246(10)	3814.5252	−0.6
	1, 2, 2 → 1, 2, 3	3814.5458(14)	3814.5365	9.3
	1, 2, 3 → 2, 3, 4	3814.5627(7)	3814.5675	−4.8
	1, 0, 1 → 2, 1, 2	3814.5874(10)	3814.5815	5.9
	1, 2, 3 → 2, 3, 2	3816.5306(12)	3816.5308	−0.2
$1_{01} \rightarrow 2_{02}$ [b]	2, 2, 2 → 2, 2, 2	7626.5389	7626.5476	−8.7
	0, 0, 0 → 1, 1, 1	7626.7736	7626.7675	6.1
	1, 1, 1 → 2, 2, 2	7627.8789	7627.8673	11.6
	2, 2, 2 → 3, 3, 3	7627.9519	7627.9615	−9.5
	1, 1, 1 → 1, 1, 1	7630.0672	7630.0667	5.2
$1_{10} \rightarrow 2_{11}$ [b]	1, 1, 1 → 2, 2, 2	7777.1674	7777.1640	3.4
	2, 2, 2 → 3, 3, 3	7778.5278	7778.5309	−3.1
	0, 0, 0 → 1, 1, 1	7779.9124	7779.9127	−0.3

[a] Fit with deuterium quadrupole interactions included.
[b] Deuterium quadrupole interactions ignored.

TABLE V. Observed and calculated unperturbed rotational line centers for four isotopic species of acetylene–HCN.

Complex	Rotational transition	Observed (MHz)	Calculated (MHz)	Difference (kHz)
$H^{12}C^{12}CH-H^{12}C^{14}N$	$0_{00} \rightarrow 1_{01}$	3 985.324	3 985.324	0
	$1_{11} \rightarrow 2_{12}$	7 847.780	7 847.794	−14
	$1_{01} \rightarrow 2_{02}$	7 970.208	7 970.207	+1
	$2_{12} \rightarrow 3_{13}$	11 771.188	11 771.199	−11
	$2_{02} \rightarrow 3_{03}$	11 954.207	11 954.207	0
	$2_{11} \rightarrow 3_{12}$	12 133.122	12 133.095	+27
	$3_{13} \rightarrow 4_{14}$	15 694.028	15 694.012	+16
	$3_{03} \rightarrow 4_{04}$	15 936.883	15 936.883	0
	$3_{12} \rightarrow 4_{13}$	16 176.518	16 176.538	−20
$H^{12}C^{12}CH-D^{12}C^{14}N$	$0_{00} \rightarrow 1_{01}$	3 982.978	3 982.980	−2
	$1_{11} \rightarrow 2_{12}$	7 843.555	7 843.578	−23
	$1_{01} \rightarrow 2_{02}$	7 965.521	7 965.521	0
	$1_{10} \rightarrow 2_{11}$	8 084.153	8 084.126	+27
	$2_{12} \rightarrow 3_{13}$	11 764.858	11 764.872	−14
	$2_{02} \rightarrow 3_{03}$	11 947.186	11 947.185	+1
	$2_{11} \rightarrow 3_{12}$	12 125.704	12 125.694	+10
	$3_{13} \rightarrow 4_{14}$	15 685.595	15 685.573	+22
	$3_{03} \rightarrow 4_{04}$	15 927.534	15 927.534	0
	$3_{12} \rightarrow 4_{13}$	16 166.647	16 166.667	−20
$H^{12}C^{12}CH-H^{12}C^{14}N$	$1_{01} \rightarrow 2_{02}$	7 826.302	...	...
	$2_{02} \rightarrow 3_{03}$	11 738.365	...	...
$D^{12}C^{12}CD-H^{12}C^{14}N$	$0_{00} \rightarrow 1_{01}$	3 814.338	...	...
	$1_{01} \rightarrow 2_{02}$	7 627.867	...	...
	$1_{10} \rightarrow 2_{11}$	7 778.264	...	...

TABLE VI. Spectral constants for four isotopic species of acetylene–HCN.

	$H^{12}C^{12}CH-H^{12}C^{14}N$	$H^{12}C^{12}CH-D^{12}C^{14}N$	$H^{13}C^{12}CH-H^{12}C^{14}N$	$D^{12}C^{12}CD-H^{12}C^{14}N$
A (MHz)	35 517(809)	35 844(817)	31 518[a]	26 896[b]
B (MHz)	2 052.988(5)	2 051.637(6)	2 012.839[a]	1 983.084[b]
C (MHz)	1 932.356(5)	1 931.362(6)	1 900.549[a]	1 831.272[b]
D_J (kHz)	4.8(2)	4.9(2)	...	...
D_{JK} (kHz)	527(6)	497(7)	...	...
χ^N_{aa} (MHz)	−4.382(2)	−4.413(2)	−4.385(17)	−4.385(11)[c] −4.399(14)[d]
χ^N_{bb} (MHz)	2.194(3)	2.206(7)	...	2.202(54)[d]
χ^N_{cc} (MHz)	2.188(4)	2.207(7)	...	2.197(55)[d]
χ^D_{aa} (kHz)	...	182(5)	...	−105(12)[c]
χ^D_{bb} (kHz)	...	−94(12)	...	...
χ^D_{cc} (kHz)	...	−88(13)	...	...

[a]Inertial defect constrained to 1.2 amu Å^2. D_J and D_{JK} constrained to $H^{12}C^{12}CH-H^{12}C^{14}N$ values.
[b]D_J and D_{JK} constrained to $H^{12}C^{12}CH-H^{12}C^{14}N$ values.
[c]Obtained in fit of $0_{00} \rightarrow 1_{01}$ transitions.
[d]Obtained in fit of $1_{01} \rightarrow 2_{02}$ and $1_{10} \rightarrow 2_{11}$ transitions.

importance of this will be discussed later. Because the deuterium nuclei lie in identical molecular environments, the two deuterium quadrupole coupling constants were constrained to be equal.

All unperturbed line centers for the four isotopic species of acetylene–HCN are given in Table V. Nuclear quadrupole coupling constants obtained from the hyperfine data in Tables I–IV along with rotational constants and centrifugal distortion constants obtained from the line centers in Table V are presented in Table VI where the numbers in parentheses represent one standard deviation in the fit. For $H^{13}C^{12}CH-H^{12}C^{14}N$ only two line centers were obtained and thus A, B, and C given in Table VI were obtained by setting D_J and D_{JK} to their values in $H^{12}C^{12}CH-H^{12}C^{14}N$ and constraining A, B, and C to the $H^{12}C^{12}CH-H^{12}C^{14}N$ inertial defect which is defined later. For $D^{12}C^{12}CD-H^{12}C^{14}N$ only three line centers were obtained and A, B, and C were fit by constraining D_J and D_{JK} to their values in $H^{12}C^{12}CH-H^{12}C^{14}N$.

B. Structure

The average and equilibrium structure of the acetylene–HCN complex is planar, T-shaped, and has C_{2v} symmetry (see Fig. 1). The HCN subunit lies along the C_2 symmetry axis with the hydrogen atom pointing midway between the triple bond of acetylene. Support of these conclusions is given by considering the rotational constants. Planarity is established by considering the inertial defect Δ defined as

$$\Delta = I^0_{cc} - I^0_{bb} - I^0_{aa}, \tag{7}$$

where I^0_{cc}, I^0_{bb}, and I^0_{aa} are the effective moments of inertia obtained from the ground vibrational state rotational constants. In the absence of vibrational motion

$$\Delta = -2\sum_i m_i c_i^2, \tag{8}$$

where c_i is the c coordinate of the ith atom and thus Δ would necessarily be 0 for a planar molecule. In weakly bound molecules with low frequency, large amplitude bending modes the inertial defect may however differ considerably from zero. In the necessarily planar complex Ar–CNCl Δ was found to be 2.75 amu Å^2, [16] and a similar value was found for $Ar-CO_2$. [17] In the present complex the inertial defect of ~1.1 amu Å^2 given in Table VII for acetylene–HCN and acetylene–DCN conclusively establishes the complex as planar.

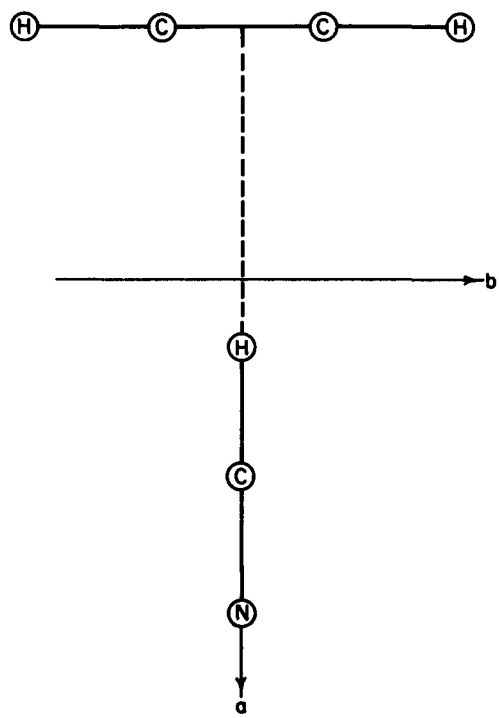

FIG. 1. The molecular geometry and identification of the principal axes of the acetylene–HCN complex.

TABLE VII. Structural parameters for four isotopic species of acetylene–HCN.

	$H^{12}C^{12}CH-H^{12}C^{14}N$	$H^{12}C^{12}CH-D^{12}C^{14}N$	$H^{13}C^{12}CH-H^{12}C^{14}N$	$D^{12}C^{12}CD-H^{12}C^{14}N$
$R_{c.m.}$ (Å)	4.216(5)	4.157(5)	...	
R_{AC-C}	3.656(5)	3.656(5)	...	
Δ(amu Å^2)	1.1(3)	1.2(3)	...	
γ(N) (deg)[a]	12.43(4)	11.69(4)	12.37(34)	12.23(25)
γ(D) (deg)[b]	...	11.9(23)	...	
θ_b (deg)[c]	8.78(6)	8.34(14)	...	
θ_c (deg)[c]	8.93(10)	8.32(14)	...	

[a]Calculated using Eq. (11) for χ_{aa}(N).
[b]Calculated using Eq. (11) for χ_{aa}(D).
[c]See the text for means of calculation.

The C_{2v} model for the structure requires that HCN lie on the C_2 symmetry axis which coincides with the a principal axis of the dimer. The contribution of HCN to the moment of inertia about the a axis and consequently to the observed A rotational constant is only through its zero-point vibrational motion. As can be shown from the vibrationally averaged angles obtained later from the nuclear quadrupole coupling constants, the two heavy atoms of HCN have vibrationally averaged displacements of ~0.09 Å from their equilibrium position on the a axis with regard to their contribution to the moment of inertia about the a axis. This compares with the acetylenic carbon and hydrogen atoms which are displaced about 0.6 and 1.2 Å, respectively. Since this moment of inertia varies with the squares of these displacements then the value of A is almost solely determined by the acetylenic atoms. Comparison of the values for A for $H^{12}C^{12}CH-H^{12}C^{14}N$ and $H^{12}C^{12}CH-D^{12}C^{14}N$ in Table VI with the free acetylene value in Table VIII shows that the a axis of the dimer must coincide with the b axis of free acetylene and establishes the C_{2v} structure.

A direct consequence of the C_{2v} symmetry is that the overall wave function ψ for $H^{12}C^{12}CH-H(D)^{12}C^{14}N$ must be antisymmetric with respect to the exchange of the two acetylenic protons. If ψ is written as a product of electronic e, vibrational v, rotational r, and nuclear n wave functions,

$$\psi = \psi_e \psi_v \psi_r \psi_n , \tag{9}$$

then it is evident that in the vibronic ground state, degeneracy of the nuclear wave function is determined by the parity of the rotational wave function. Arguments given elsewhere[2,3] regarding the symmetry of rotational wave functions and the degeneracies of symmetric and antisymmetric nuclear wave functions lead to a 3:1 enhancement for $K_{-1}=1$ lines compared to $K_{-1}=0$ lines over the normal line strength factors for $H^{12}C^{12}CH-$

TABLE VIII. Molecular constants for isotopic species of free HCN and acetylene.

	$H^{12}C^{14}N$	$D^{12}C^{14}N$	$H^{12}C^{12}CH$	$D^{12}C^{12}CD$
b(MHz)	44 315.975(4)[a]	36 207.4627(a)[a]	35 455.53[b]	25 419.0[b]
r_s (H–C) (Å)	1.063 17[c]			
r_s (C–N) (Å)	1.155 38[c]			
r_e (H–C) (Å)			1.062 50(10)[b]	
r_e (C–C) (Å)			1.202 41(9)[b]	
$\alpha_{\parallel CN}$(Å^3)	3.1[d]			
χ_0^N (MHz)	−4.709 1(13)[a]	−4.7030(12)[a]		
χ_0^D (kHz)		194.4(22)[a]		
μ (10^{-18} SC cm)	2.985[e]			
Θ(10^{-26} SC cm^2)	3.1(6)[f]		8.39[f]	
Φ(10^{-42} SC cm^4)			2.18[g]	

[a]F. C. deLucia and W. Gordy, Phys. Rev. A **187**, 58 (1969).
[b]E. Kostyk and H. L. Welsh, Can. J. Phys. **58**, 912 (1980).
[c]C. C. Costain, J. Chem. Phys. **29**, 864 (1958).
[d]K. G. Denbigh, Trans. Faraday Soc. **36**, 936 (1940).
[e]A. G. Maki, J. Chem. Phys. Ref. Data 3, 221 (1974).
[f]S. L. Hartford, W. C. Allen, C. L. Norris, E. F. Pearson, and W. H. Flygare, Chem. Phys. Lett. **18**, 153 (1973).
[g]R. D. Amos and J. H. Williams, Chem. Phys. Lett. **66**, 471 (1979).

H(D)CN. Though our spectrometer does not give quantitative intensity information, these effects were seen qualitatively with the effect that all $K_{-1}=1$ lines were stronger than $K_{-1}=0$ lines though the normal line strength factor predicts otherwise. The deuterium quadrupole split $J=1\rightarrow 2$ transitions were measured approximately during the same time period for both acetylene–DCN and a similar complex ethylene–DCN[18] which has opposite overall parity and thus $K_{-1}=0$ lines are enhanced 5:3. Measurement of 20–30 hyperfine components in each complex clearly showed the $K_{-1}=1$ lines to be stronger than the $K_{-1}=0$ lines in the acetylene–DCN complex with opposite results in the ethylene–DCN complex. This observation is unexplainable without consideration of nuclear spin statistics as the normal line strength factor is the same in both complexes.

Further evidence for the observation of the effects of nuclear spin statistics is the absence of all transitions originating in the $J=0$, $F_2=1$ state from the observed $0_{00}\rightarrow 1_{01}$ spectrum of D ^{12}C ^{12}CD–H ^{12}C ^{14}N where the basis is described in Eq. (5). Since in this isotopic species two bosons are exchangeable by a C_2 symmetry operation about the a axis, the overall wave function given in Eq. (9) must be symmetric with respect to this operation. This will eliminate all antisymmetric nuclear spin states from existing in the symmetric 0_{00} rotational state where the nuclear spin state is defined in terms of the total spin of the deuterium nuclei. It is easily shown for two identical $I=1$ nuclei that the nuclear spin state is symmetric for $I_{\text{total}}=0,2$ and antisymmetric for $I_{\text{total}}=1$. For the $J=0$ rotational state and the basis given in Eq. (5) the F_2 quantum number will be equivalent to the total deuterium nuclear spin. Therefore, all states with $J=0$, $F_2=1$ will be nonexistent for this isotopic species under the assumption of C_{2v} symmetry.

The rotational constants obtained for H ^{13}C ^{12}CH–H ^{12}C ^{14}N and D ^{12}C ^{12}CD–H ^{12}C ^{14}N also reinforce the proposed structure. The B and C values for these isotopic species are within a few MHz of those calculated using a rigid structure. This level of error has been found to be common in fitting a rigid structure to rotational constants in these loosely bound asymmetric rotors where large amplitude bending modes are produced upon complexation. Though no standard deviation is available for the A rotational constant in D ^{12}C ^{12}CD–H ^{12}C ^{14}N it is slightly larger than the rotational constant of free D ^{12}C ^{12}CD given in Table VIII. This is most likely due to the in-plane bending motion of acetylene with respect to HCN. This will effectively decrease I^0_{aa} and thus increase the observed value of A slightly.

The distance $R_{\text{c.m.}}$ between the centers of mass of the subunits can be calculated from the B and C rotational constants. Since $\langle 1/I^0_{gg}\rangle$ $(g=b,c)$ is determined from the rotational constants, where I^0_{gg} is the moment of inertia in the ground vibrational state, we first make the approximation

$$\left\langle \frac{1}{I^0_{gg}} \right\rangle = \frac{1}{\langle I^0_{gg}\rangle} \quad , \quad g=b,c \ . \tag{10}$$

Secondly, since $\langle I^0_{gg}\rangle$ $(g=b,c)$ depends upon $\langle g_i^2\rangle$ $(g=a,b,c)$ where g_i is a principle axis coordinate for the ith atom, we have to assume $\langle g_i^2\rangle=\langle g_i\rangle^2$ $(g=a,b,c)$ when no vibrational information is present. We have no vibrational information about the acetylene subunit and will have to neglect these effects in fitting $R_{\text{c.m.}}$ to B and C. We do, however, have some information about the large amplitude vibrational motion of H(D)CN off the a axis. If for the moment we neglect changes in the environment of N and D upon complexation in acetylene–HCN and acetylene–DCN we can represent χ^{N}_{aa} and χ^{D}_{aa} as

$$\chi^i_{aa}=\tfrac{1}{2}\chi^i_0\langle 3\cos^2\zeta-1\rangle \ , \quad i=\text{N},\text{D} \ , \tag{11}$$

where ζ is the instantaneous angle between C≡N and the a axis of the dimer if $i=$N and between D–C and the a axis if $i=$D. χ^i_0 is the free coupling constant of nitrogen in HCN or DCN if $i=$N or of deuterium in DCN if $i=$D and is given in Table VIII, and the brackets indicate averaging over the ground state vibrational wave function. From Eq. (11) we may obtain an operationally defined angle γ for γ^{N}_{aa} and χ^{D}_{aa} for the various isotopic species of acetylene–HCN, where

$$\gamma=\arccos\langle\cos^2\zeta\rangle^{1/2} \ . \tag{12}$$

The acute values for γ are taken for reasons to be discussed shortly. These angles are listed in Table VII with their uncertainties σ_γ given analytically by

$$\sigma_\gamma=\frac{\left(\frac{180}{\pi}\right)\left[\sigma^2_{\chi_{aa}}+\frac{\chi_{aa}}{\chi_0}\sigma^2_{\chi_0}\right]^{1/2}}{\left[1-\left(\frac{2\chi_{aa}}{3\chi_0}+1/3\right)^2\right]^{1/2}\left(\frac{2\chi_{aa}}{3\chi_0}+1/3\right)^{1/2}3\chi_0} \ . \tag{13}$$

The agreement within experimental uncertainty of γ obtained from χ^{N}_{aa} and from χ^{D}_{aa} in acetylene–DCN indicates we can probably treat H(D)CN as a rigid subunit for the present calculation. The six instantaneous moment of inertia tensor elements can then be derived in terms of the moments of inertia of HCN and acetylene and the parameters $R_{\text{c.m.}}$, γ[given in Eq. (12)], and β shown in Fig. 2. Since $\chi^{\text{N}}_{bb}=\chi^{\text{N}}_{cc}$ within experimental error then under the present assumption of unchanged electronic environment at N we can average isotropically over the β dependence,

$$\frac{1}{2\pi}\int_0^{2\pi} I(R_{\text{c.m.}},\gamma,\beta)_{ij}\,d\beta=I(R_{\text{c.m.}},\gamma)_{ij}, \quad i,j=x,y,z \ . \tag{14}$$

This results in all off-diagonal elements equaling zero and gives for I_{bb} and I_{cc}:

$$I_{bb}=I_{\text{acet}}+I_{\text{PD}}+I_{\text{HCN}}\tfrac{1}{2}(1+\cos^2\gamma) \ , \tag{15}$$

$$I_{cc}=I_{\text{PD}}+I_{\text{HCN}}\tfrac{1}{2}(1+\cos^2\gamma) \ .$$

I_{PD} is the pseudodiatomic moment of inertia given by

$$I_{\text{PD}}=\frac{M_{\text{HCCH}}M_{\text{HCN}}}{M_{\text{HCCH}}+M_{\text{HCN}}}R^2_{\text{c.m.}} \ . \tag{16}$$

We then fit $R_{\text{c.m.}}$ in both isotopes using values for γ from Table VII. The resultant values of $R_{\text{c.m.}}$ are given in Table VII along with the acetylene carbon distances, $R_{\text{Ac–C}}$, which are shown to be constant in both isotopes. This reflects the fact that the change in $R_{\text{c.m.}}$ from acetylene–HCN to acetylene–DCN corresponds almost exactly to the change in the center of mass of HCN in going to DCN.

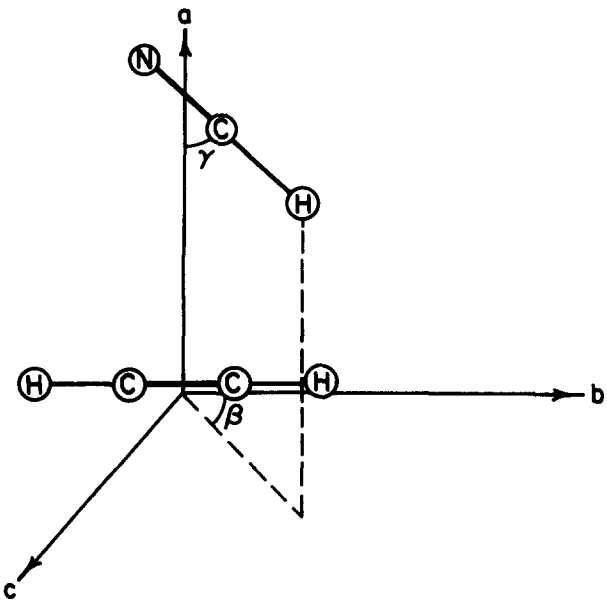

FIG. 2. The structure of the acetylene–HCN complex. The angles α and β are vibrational coordinates. The average value of these coordinates is zero.

In taking the acute values for the angles γ obtained from Eq. (11) it has been assumed that the complex is hydrogen bonded like the analogous dimers acetylene–HF[6] and acetylene–HCl[2] rather than antihydrogen bonded like HF–Cl_2[19] and HF–ClF.[20] This is easily shown by considering $R_{c.m.}$ for both isotopes which could have been calculated within the uncertainty of the values in Table VII without knowledge of the orientation of HCN. By ignoring HCN zero-point vibrations out of plane and using the equation for a planar molecule

$$I_{cc} = I_{HCN} + I_{HCCH} + I_{PD} \ . \tag{17}$$

$R_{c.m.}$ is calculated to be 4.219 and 4.160 Å for acetylene–HCN and acetylene–DCN, respectively. Since $R_{c.m.}$ calculated here is 0.059 Å shorter for acetylene–DCN and since the center of mass in DCN is 0.059 Å farther from nitrogen than in HCN the antihydrogen-bonded model requires that N in H(D)CN be 0.118 Å closer to acetylene in the acetylene–DCN dimer than in the acetylene–HCN dimer. This is unreasonable and discounts the antihydrogen-bonded possibility.

C. Interpretation of the nuclear quadrupole coupling constants

The previous assumption of unchanged nuclear environments upon complexation will now be examined. Previous work on N_2–HF,[21] NCCN–HF,[22] CH_3CN–HF,[23] and HCN–HCN[10] has shown that effects other than second rank tensor projection as described by Eq. (11) contribute to the measured nuclear quadrupole coupling constants in many of these loosely bound complexes. The long range effects of the presence of acetylene on the electric field gradient (EFG) experienced at the nitrogen nucleus can be obtained by considering the potential $V(r, \theta)$, at a given point due to acetylene

$$V(r, \theta) = \frac{\Theta P_2(\cos\theta)}{r^3} + \frac{\Phi P_4(\cos\theta)}{r^5} \cdots , \tag{18}$$

where Θ and Φ are the molecular electrostatic quadrupole and hexadecapole moments of acetylene, $P_2(\cos\theta)$ and $P_4(\cos\theta)$ are Legendre polynomials, and all odd moments are 0 due to symmetry. Since the nitrogen atom lies on average on the a axis, the EFG experienced by the nitrogen nucleus directly as a result of the multipole moments of acetylene, with a correction for the Sternheimer shielding phenomenon,[24] is given by

$$q^N = (1-\gamma^N)\left\langle \frac{\partial^2 v}{\partial a^2} \right\rangle$$

$$= (1-\gamma^N)\left\langle \frac{12\Theta P_2(\cos\theta)}{r^5} + \frac{30\Phi P_4(\cos\theta)}{r^7} \cdots \right\rangle \ . \tag{19}$$

We will calculate expressions for $P_n(\theta)$ in Eq. (19) algebraically using $\theta = 90°$. Using the values of Θ and Φ from Table VIII, $\gamma^N = +3$ for N in HCN,[25] $r = 4.812$, and

$$\chi = \frac{|e|qQ^N}{h} , \tag{20}$$

where e is the fundamental charge and Q^N is the nuclear quadrupole moment of nitrogen taken to be 1.93×10^{-26} cm^2,[26] we obtain a contribution of +5 kHz to the observed value of χ^N_{aa} for this effect in H ^{12}C ^{12}CH–H ^{12}C ^{14}N and H ^{12}C ^{12}CH–D ^{12}C ^{14}N. The second term of Eq. (19) is 2% of the first.

A greater contribution to the observed value of χ^N_{aa} is likely to come about as a result of polarization of C≡N by the electric field generated by the acetylene subunit whereby N becomes slightly more negative in charge. This contribution, χ^{pol}_{aa}, to the observed coupling constant can be expressed as

$$\chi^{pol}_{aa} = \left(\frac{\partial\chi^N_{aa}}{\partial E}\right)\left[\frac{3\Theta P_2(\cos\theta)}{r^4} + \frac{5\Phi P_4(\cos\theta)}{r^5} \cdots\right] , \tag{21}$$

where $(\partial\chi^N_{aa}/\partial E)$ is the first order change in χ^N_{aa} resulting from charge rearrangement within H(D)CN occurring in an axial field and the series in parenthesis represents the electric field at the C≡N center of mass resulting from acetylene. Calculations for HCN give 0.87 MHz/(D/Å^3)[25] for $(\partial\chi^N_{aa}/\partial E)$ however a value can also be calculated within the limitations of simple Townes–Dailey arguments[27] in the following manner. We first interpret the dipole induced in C≡N as a result of fractional transfer of an electron from the $2p_x$ or $2p_y$ tranverse atomic orbitals of C into the corresponding orbitals at N. χ^{pol}_{aa} is then given by

$$\chi^{pol}_{aa} = \frac{\mu_{ind}}{R_{CN}|e|}\chi_{2p_x} , \tag{22}$$

where χ_{2p_x} is the change in χ^N_{aa} experienced with the addition of one electron to the nitrogen $2p_x$ orbital. χ_{2p_x} has been calculated as 4.9 MHz for the HCN molecule[28] but can be calculated for the nitrogen atom by using

$$\chi_{2p_x} = \frac{e^2Q^N}{h}\frac{2}{5}\left\langle\frac{1}{r^3}\right\rangle_{2p_x} . \tag{23}$$

Using $\langle 1/r^3\rangle_{2p_x}$ of 22.5×10^{24} cm^{-3} [29] gives 6.0 MHz which serves only to confirm the validity of the first value. By noting that χ^{pol}_{aa} is the only field-dependent contribution to χ^N_{aa}, we differentiate Eq. (22) with respect to E and obtain

$$\left(\frac{\partial \chi_{aa}}{\partial E}\right)=\frac{4.9\ \text{MHz}}{R_{CN}|e|}\left(\frac{\partial \mu_{ind}}{\partial E}\right)=\frac{4.9\ \text{MHz}}{R_{CN}|e|}\alpha_{CN}\,, \tag{24}$$

where α_{CN} is the parallel polarizability of CN. Using values in Table VIII for α_{CN} and R_{CN} we obtain 2.7 MHz/(D/Å^3) for $(\partial\chi_{aa}/\partial E)$ which is about three times the previous value given. Using the two values as lower and upper limits, substitution into Eq. (21) gives 32–100 kHz for acetylene–H(D)CN where now $r=4.278$ Å.

In summary then, the major contribution to the observed value of χ^N_{aa} in acetylene–H(D)CN is given by tensor projection described by Eq. (11) with polarization accounting for 1%–2% of the observed value. The angles thus derived from χ^N_{aa} to describe the zero-point vibrational motion of C≡N away from the a axis in acetylene–H(D)CN are no more than 2° too high.

We now examine the deuterium nuclear quadrupole coupling in H ^{12}C ^{12}CH–D ^{12}C ^{14}N. The long range effects described by Eq. (19) as applied to deuterium can be calculated using $\gamma^0=0.33$,[30] $Q^N=2.86\times10^{-27}$ cm^2,[31] and $r=2.593$ Å to give −6 kHz. Polarization of the D–C bond is estimated to be four times smaller than for C≡N[32] and thus polarization effects on χ^D_{aa} might at first be expected not to be severe. However, any attempt to verify this by simple calculation is frustrated by the inapplicability of Townes–Dailey theory here. The situation is further complicated since the aforementioned polarization of C≡N by acetylene will be nonnegligible in terms of its effect on the EFG at the deuteron and also since some bond elongation of the D–C bond may occur. For these reasons further analysis of χ^D_{aa} for H ^{12}C ^{12}CH–D ^{12}C ^{14}N will not be attempted. The value obtained for χ^D_{bb} indicates isotropy in the EFG experienced at deuterium however the uncertainty of 12 kHz precludes any definitive statements.

In considering χ^D_{aa} obtained for D ^{12}C ^{12}CD–H ^{12}C ^{14}N it is unlikely there is significant polarization near the sites of the deuterium nuclei. Furthermore, the long range effects of HCN on χ^D_{aa} by an equation similar to Eq. (19) with the addition of a dipole term and utilizing information in Table VIII are negligible. Therefore any changes in χ^D_{aa} in the dimer from χ^D_{bb} in free D ^{12}C ^{12}CD are likely a result of Eq. (11) or quantum mechanical changes in the subunits upon complexation. Values for χ^D_{bb} in D–C≡C–R are in fact very consistent with χ^D_{bb} equaling −106(4), −105(1), −100(5), and −104(5) kHz for R = F,[33] R = Cl,[34] R = D,[35] and R = CH$_3$,[33] respectively. The agreement between the observed value of χ^D_{aa} in D ^{12}C ^{12}CD–H ^{12}C ^{14}N and these values indicates that the net contribution of vibrational effects and quantum mechanical changes to χ^D_{aa} are not greater than the uncertainty in the value.

IV. DISCUSSION

The binding of acetylene–HCN will now be considered in terms of both binding strength and bending motion of HCN. It has been shown[8] that to a good level of approximation the relationship between D_J and the hydrogen bond stretching force constant k_s in this and other asymmetric rotor complexes is given by

TABLE IX. Comparison of binding parameters for the acetylene–HCN and acetylene–HCl dimers.

	Acetylene–HCN	Acetylene–HCl
k_s (mdyn/Å)	0.053	0.067
ν_s (cm^{-1})	82	87
ϵ (cm^{-1})	642	614
$R_{\text{acet–HA}}$	3.656	3.699
γ (deg)	12.43(4)	21.21(1)
θ_b (deg)	8.1(2)	15.69(1)
θ_c (deg)	8.2(2)	15.00(2)

$$k_s=\frac{8\pi^3(\mu_{PD}R_0)^2[(B^2+C^2)^2+2(B^4+C^4)]}{\hbar D_J}\,. \tag{25}$$

μ_{PD} is the pseudodiatomic reduced mass defined as

$$\mu_{PD}=\frac{M_{HCN}M_{HCCH}}{M_{HCN}+M_{HCCH}}\,. \tag{26}$$

From k_s a well depth ϵ for the hydrogen-bond interaction can be obtained using a standard procedure which utilizes a Lennard-Jones 6-12 potential and a pseudodiatomic model.[13] k_s, ϵ, and ν_s, the hydrogen-bond stretching frequency are given in Table IX for the H ^{12}C ^{12}CH–H ^{12}C ^{14}N isotopic species and is compared to acetylene–HCl which has a similar well depth. Also given is $R_{\text{acet–HA}}$ which is the distance between acetylene and the first heavy atom of its binding partner. It is apparent that these two C_{2v} dimers are similar in both ϵ and $R_{\text{acet–HA}}$.

Though the angles derived from the quadrupole coupling constants have a certain amount of error as discussed previously owing to electronic rearrangement and electrostatic interactions, they do undeniably provide some insight into the zero-point vibrational motion. For instance, the smaller angle derived from χ^N_{aa} in acetylene–DCN as compared to that obtained in acetylene–HCN clearly shows that the heavier deuteron is attenuating the zero-point vibrational bending motion of C≡N as all charge rearrangement and electrostatic contributions to χ^N_{aa} are the same in both isotopic species. The much smaller value of γ obtained from χ^N_{aa} in acetylene–HCN as compared to γ obtained from χ^{Cl}_{aa} in the analagous acetylene–HCl dimer, as shown in Table IX, can be explained similarly. The bending motion of the binding partner of acetylene about its center of mass is attenuated more in acetylene–HCN by the carbon and nitrogen atoms than in acetylene–HCl where this motion involves a near stationary Cl atom.

It is interesting to compare the value of γ obtained from χ^N_{aa} for acetylene–HCN with values obtained for other hydrogen-bound systems involving HCN as a proton donor or proton acceptor as illustrated in Table X. In HCN–HCl[11] and HCN–HBr[12] where HCN is a proton acceptor, γ is 17°–18°. A similar value of γ of 17° is obtained for the proton acceptor HCN in $(HCN)_2$.[10] However, when HCN serves as a proton donor in $(HCN)_2$, ethylene–HCN, and acetylene–HCN γ is 11°–13°. The consistency in these values indicates that HCN probably

TABLE X. Comparison of values for γ obtained from χ_{aa}^{N} in hydrogen-bonded dimers involving HCN.

HCN as a proton acceptor:	
Complex	γ (deg)
HCN–HCl[a]	17
HCN–HBr[b]	18
HCN–HCN[c]	17
HCN as a proton donor:	
Complex	γ (deg)
Acetylene–HCN	12
Ethylene–HCN[d]	13
HCN–HCN[c]	11

[a]Reference 11. [c]Reference 10.
[b]Reference 12. [d]Reference 18.

experiences a narrower bending potential when serving as a proton donor than as a proton acceptor.

Another comparison of interest in considering the analagous C_{2v} dimers acetylene–HCl and acetylene–HCN, is the angular information obtained from the Cl and N quadrupole coupling constants when broken down to in-plane and out-of-plane bending angles where these reflect γ projected into the *ab* and *ac* planes, respectively. The projection of the free HCN nitrogen coupling constant tensor into the principal axis system of the dimers requires rotation through two Euler angles α and β. If the z axis in the free HCN principal axis system is first rotated into the *ab* plane of the dimer by the euler angle α and then into the a axis by a rotation through β, we have

$$\chi_{aa} = (3/2\cos^2\beta\cos^2\alpha - 1/2)\chi_0 ,$$
$$\chi_{bb} = (3/2\sin^2\beta\cos^2\alpha - 1/2)\chi_0 , \quad (27)$$
$$\chi_{cc} = (3/2\sin^2\alpha - 1/2)\chi_0 .$$

By relating α and β to the in-plane and out-of-plane angles θ_b and θ_c, respectively, we obtain

$$\theta_g = \arccos\left[\left(\frac{\chi_{aa} + \chi_0/2}{\chi_{aa} + \chi_0 + \chi_{gg}}\right)\right]^{1/2}, \; g = b, c . \quad (28)$$

For acetylene–HCl χ_{bb} and χ_{cc} differ in the three isotopes studied by 0.5 MHz or more translating into θ_b being greater than θ_c by almost one degree with uncertainty of 0.01° as shown in Table X. In acetylene–HCN no such anisotropy is present as shown by θ_b and θ_c in Table X as $\chi_{bb} = \chi_{cc}$ within experimental error.

[1]A. C. Legon, P. D. Aldrich, and W. H. Flygare, J. Am. Chem. Soc. **102**, 7584 (1980).
[2]A. C. Legon, P. D. Aldrich, and W. H. Flygare, J. Chem. Phys. **75**, 625 (1981).
[3]P. D. Aldrich, A. C. Legon, and W. H. Flygare, J. Chem. Phys. **75**, 2126 (1981).
[4]L. W. Buxton, P. D. Aldrich, J. A. Shea, A. C. Legon, and W. H. Flygare, J. Chem. Phys. **75**, 2681 (1981).
[5]A. C. Legon, P. D. Aldrich, and W. H. Flygare, J. Am. Chem. Soc. **104**, 1486 (1982).
[6]W. G. Read and W. H. Flygare, J. Chem. Phys. **76**, 2238 (1982).
[7]J. A. Shea and W. H. Flygare, J. Chem. Phys. **76**, 4857 (1982).
[8]W. G. Read, E. J. Campbell, and Giles Henderson, J. Chem. Phys. (in press).
[9]P. D. Aldrich and E. J. Campbell, Chem. Phys. Lett. **93**, 355 (1982).
[10]L. W. Buxton, E. J. Campbell, and W. H. Flygare, Chem. Phys. **56**, 399 (1981).
[11]A. C. Legon, E. J. Campbell, and W. H. Flygare, J. Chem. Phys. **76**, 2267 (1982).
[12]E. J. Campbell, A. C. Legon, and W. H. Flygare, J. Chem. Phys. (in press).
[13]T. J. Balle, E. J. Campbell, M. R. Keenan, and W. H. Flygare, J. Chem. Phys. **71**, 2723 (1979); **72**, 922 (1980).
[14]T. J. Balle and W. H. Flygare, Rev. Sci. Instrum. **52**, 33 (1981).
[15]E. J. Campbell, L. W. Buxton, T. J. Balle, M. R. Keenan, and W. H. Flygare, J. Chem. Phys. **74**, 829 (1981).
[16]M. R. Keenan, D. B. Wozniak, and W. H. Flygare, J. Chem. Phys. **75**, 631 (1981).
[17]J. M. Steed, T. A. Dixon, and W. Klemperer, J. Chem. Phys. **70**, 4095 (1979).
[18]S. G. Kukolich, W. G. Read, and P. D. Aldrich, J. Chem. Phys. (in press).
[19]F. A. Baiocchi, T. A. Dixon, and W. Klemperer. Ohio State Symposium on Molecular Spectroscopy, RC3 (1981).
[20]S. E. Novick, K. C. Janda, and W. Klemperer, J. Chem. Phys. **65**, 5115 (1976).
[21]P. D. Soper, A. C. Legon, W. G. Read, and W. H. Flygare, J. Chem. Phys. **76**, 292 (1982).
[22]A. C. Legon, P. D. Soper, and W. H. Flygare, J. Chem. Phys. **74**, 4936 (1981).
[23]P. D. Soper, A. C. Legon, W. G. Read, and W. H. Flygare, J. Phys. Chem. **85**, 3440 (1981).
[24]R. Sternheimer, Phys. Rev. **80**, 102 (1950); **84**, 244 (1951); **86**, 316 (1952), **95**, 736 (1954).
[25]S. Engström, H. Wennerström, Bo Jönsson, and G. Karlström, Mol. Phys. **34**, 813 (1977).
[26]H. Winter and H. J. Andrä, Phys. Rev. A **21**, 581 (1980).
[27]C. H. Townes and B. P. Dailey, J. Chem. Phys. **17**, 782 (1949).
[28]R. Bonaccorsi, E. Scrocco, and J. Tomasi, J. Chem. Phys. **50**, 2940 (1969).
[29]C. H. Townes and A. L. Schawlow, *Microwave Spectroscopy* (Dover, New York, 1955).
[30]F. D. Feiock and W. R. Johnson, Phys. Rev. **187**, 39 (1969).
[31]R. V. Reid and M. L. Vaida, Phys. Rev. Lett. **34**, 1064 (1975); **29**, 494 (1972).
[32]K. G. Denbigh, Trans. Faraday Soc. **36**, 936 (1940).
[33]V. Weiss and W. H. Flygare, J. Chem. Phys. **45**, 8 (1966).
[34]C. D. Cogley, L. M. Task, and S. G. Kukolich, J. Chem. Phys. **76**, 5669 (1982).
[35]J. N. Pinkerton, thesis, Harvard University, 1961.